DOI: 10.1002/chem.200601726

A Concerted Approach for the Determination of Molecular Conformation in Ordered and Disordered Materials

Jan Sehnert and Jürgen Senker*[a]

Abstract: We present the successful application of a concerted approach for the investigation of the local environment in ordered and disordered phases in the solid state. In this approach we combined isotope labeling with computational methods and different solid-state NMR techniques. We chose triphenylphosphite (TPP) as an interesting example of our investigations because TPP exhibits two crystalline modifications and two different amorphous phases one of which is highly correlated. In particular we analyzed the conformational distribution in three of these phases. A sample of triply labeled 1-[^{13}C]TPP was prepared and 1D MAS as well as wide-line ^{13}C NMR spectra were measured. Furthermore we acquired 2D ^{13}C wide-line exchange spectra and used this method to derive highly detailed information about the phenyl orientation in the investigated TPP phases. For linkage with a structure model a DFT analysis of the TPP molecule and its immediate environment was carried out. The ab initio calculations of the ^{13}C chemical shift tensor in three- and six-spin systems served as a base for the calculation of 1D and 2D spectra. By comparing these simulations to the experiment an explicit picture of all phases could be drawn on a molecular level. Our results therefore reveal the high potential of the presented approach for detailed studies of the mesoscopic environment even in the challenging case of amorphous materials.

Keywords: ab initio calculations · chemical shift anisotropy · solid-state NMR spectroscopy · structure elucidation

Introduction

Up to today structure investigations in liquids and glasses prove a challenging task. In particular information from the intermediate range of 10–100 Å is needed to understand glass structures, nucleation and growth mechanisms, self-organization and phenomena such as polymorphism or polyamorphism.[1–5] In this work we will show for triphenylphosphite (TPP) that by choosing a combination of solid-state NMR spectroscopy, computer simulation and isotope labeling detailed structure investigations down to the molecular level become feasible even in amorphous or disordered systems.

Due to substantial progress in both the technical development of NMR spectroscopy and the ab initio calculation of the full chemical shift interaction solid-state NMR serves as an especially powerful tool of analysis in the mesoscopic regime. By combining computational and experimental results today it is even possible to extract structural data from NMR experiments sensitive to the orientation of the chemical shift tensor. This is a non-trivial task because it requires knowledge about the orientation of the NMR tensor towards characteristic building blocks of the system. Beside rotation pattern measurements for single crystals quantum mechanical calculations serve as the only source for this kind of information.[6–8]

With the most commonly used gauge including atomic orbital (GIAO) method[9] NMR tensors can be computed with high accuracy in a reasonable time frame. In the last decade research based on an approach of combined computational and solid-state NMR methodology showed that there is a close relation between NMR tensors and structure.[10–15] This correlation has been used to investigate structural features like for example configuration,[16–20] hydrogen bonding[21,22] or even intermolecular arrangement[23] in the solid state. For a description of the tensor in condensed phases the polarizable continuum model,[24,25] embedded cluster methods[22,24] and computations under full periodic boundary conditions using plane waves[26–29] have been used most recently. All these fundamental studies show that the interplay of solid-state NMR and ab initio calculations has improved to an extent that now it is widely accepted to yield structural in-

[a] J. Sehnert, Prof. Dr. J. Senker
Anorganische Chemie I, Universität Bayreuth
Universitätsstrasse 30, 95447 Bayreuth (Germany)
Fax: (+49) 921-55-2788
E-mail: juergen.senker@uni-bayreuth.de

 © 2007 Wiley-VCH Verlag GmbH & Co. KGaA, Weinheim WILEY InterScience DISCOVER SOMETHING GREAT

formation on a nanoscopic scale.[30] However, most of the above-mentioned work dealt with already known crystalline systems. Frequently structure models obtained from X-ray or neutron diffraction data have been used. Up to now there are only a few NMR investigations in disordered condensed phases which apply computational models for structure proposal.[26,31–33]

We now extend the use of ab initio calculations to a concerted approach for structural investigations in arbitrary ordered and disordered materials. This approach is based on a combination of isotope labeling, ab initio calculations and solid-state NMR spectroscopy. In this strategy structure proposals are generated using molecular modeling methods (DFT, semiempirical or force field methods). Such structures then provide a basis for the ab initio calculation of NMR tensors and thereby a fully ab initio simulation of NMR spectra which can be compared with experimentally obtained data.

Whereas in a majority of cases only the isotropic chemical shift is taken into account for structural analysis we focus on the anisotropic properties of the chemical shift interaction, especially the tensor orientation. This is advantageous in terms of the computational effort since it is known that tensor orientations can be calculated with high accuracy at low costs.[25,34–37] Furthermore in previous works it was shown that the orientation correlation of NMR tensors can efficiently be applied to investigate structure in ordered and disordered phases.[38,39] A limitation of this method was that usually the orientation of the tensor towards the structural building block was unknown and could only be estimated. With the inclusion of ab initio calculations a direct interpretation of the spectra in terms of a proposed structure model becomes feasible. On this base radio-frequency-driven spin-diffusion spectroscopy can be transferred to arbitrary spin-$^1/_2$ systems and the full range of organic solid-state systems is accessible to detailed structural NMR investigations. In addition to that synthetic isotope labeling serves as a tool to specifically pick out molecular domains. This influence over the investigated spin system gives the approach a great amount of flexibility.

Results and Discussion

Triphenylphosphite: Triphenylphosphite (TPP) poses an interesting example for our investigations. Even though built up by a small molecule (see Figure 1) the accessible solid-state phases include two different crystalline (c1[40] and c2[41]) and two amorphous states (aI and aII).[39] Of the crystalline phases c1 is the commonly found modification whereas c2 can only be crystallized from an ionic liquid.[41] The amorphous phases can be distinguished between the structural glass (aI with $T_g = 205$ K) and the second phase aII which is produced via annealing the supercooled liquid in a temperature range of $210 \leq T_a \leq 230$ K.[39] This latter phase contains highly correlated domains which have been investigated with ^{31}P rf-driven spin diffusion spectroscopy.[39]

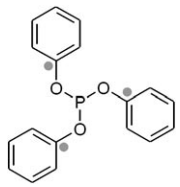

Figure 1. Tri-(1-[^{13}C]phenyl)-phosphite.

Strong evidence was found that the domains consist of clusters a few molecules in size and parallely arranged as seen in the crystalline phase c1. Furthermore, very recently the nature of the phase transformation from aI to aII has been associated with a change in molecular conformation and the demand for the elucidation of the structure on a microscopical regime has been corroborated.[42]

We therefore want to apply the concerted approach to a conformational analysis of the TPP phases aI, aII and c1. For our measurements we synthesized tri-(1-[^{13}C]phenyl)-phosphite. The intramolecular correlation was separated by choosing appropriate mixing times in the rf-driven spin-diffusion experiment. Computationally a conformational description of the TPP system was performed with DFT methods which yield accurate structure models. On that base system sizes up to a maximum of two molecules can be treated.

In the above-mentioned picture the respective phases should be well distinguishable. The glassy phase aI contains a broad distribution of possible conformers. Upon clustering in phase aII it should significantly narrow down to a small distribution about one preferential conformer which resembles the molecular structure found in the crystalline phase c1. Finally in phase c1 only the crystalline conformer is present.

TPP conformers: Figure 2 shows the minima for the conformational study of a single molecule. An overall of eight structures could be found for B3LYP and the use of the 6-31G(d) and 6-31+G(d,p) basis sets. Except for VI and VII both basis sets result in similar structures. Minimum VI is found with 6-31+G(d,p) and transforms into conformer IV upon optimization with 6-31G(d). Structure VII is stable with 6-31G(d) but transforms into conformer VIII with the 6-31+G(d,p) basis set. Minimum I exhibits C_s symmetry whereas VIII is C_3 symmetric. In structure III the C_s symmetry is broken by a slight tilt of the C2 phenyl ring.

It is noteworthy that structures could be found which resemble the crystalline polymorphs c1 (I, Figure 2) and c2 (II, Figure 2). For both the geometry optimization of a single molecule taken from the X-ray structures reproduce the results. In minimum I the overall maximum deviations from the X-ray structure for bond lengths are 0.02 Å, 1° for angles and 2° for dihedral angles. H atoms are excluded from these observations as their positions are not well described through X-ray methods. Bigger differences up to 16° for dihedral angles occur where packing effects account for a distortion of the phenyl rings.[40] As expected gas-phase

 © 2007 Wiley-VCH Verlag GmbH & Co. KGaA, Weinheim

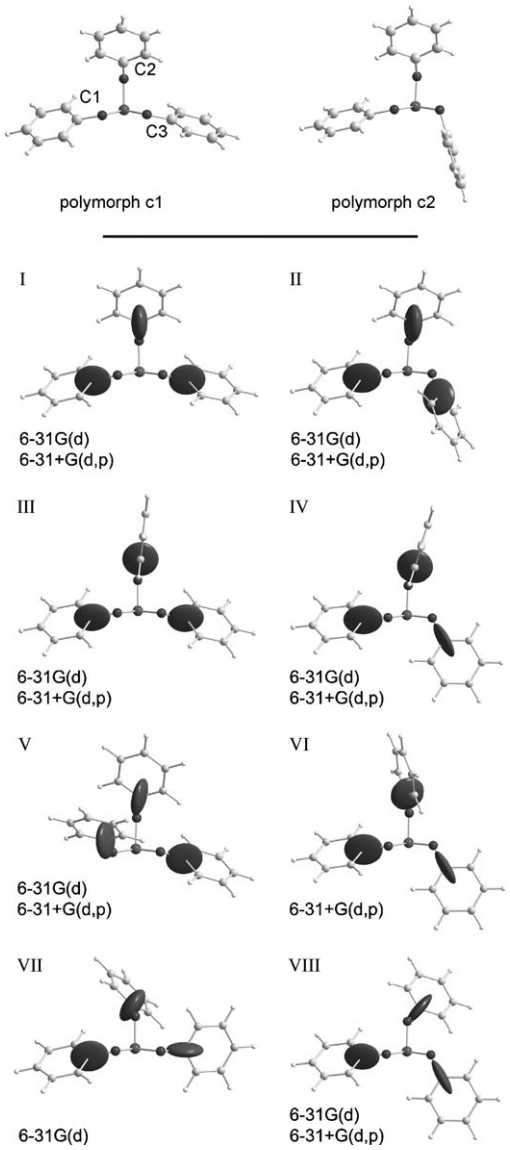

Figure 2. Top: Conformers of the crystalline phases c1[40] and c2;[41] Bottom: DFT calculated minimum structures; ^{13}C ab initio anisotropies are depicted as tensor ellipsoids for the labeled positions (see also Figure 1).

optimizations of polymorph c1 do not reproduce this feature and always result in C_s symmetry (compare the phenyl rings C1 and C3 of structures c1 and I in Figure 2). For c2 the comparison between experiment and calculation in general shows deviations of 0.01–0.05 Å for bond lengths, 1° for angles and 1° for dihedral angles. Again greater differences occur where phenyl rings are distorted due to packing effects (see phenyl rings C2 and C3 in structures c2 and II of Figure 2). In this case deviations in dihedral angles of up to 28° are found. The gas-phase structures of single TPP molecules calculated with B3LYP seem to reproduce experimental structures well with the exception of the torsion of phenyl rings due to crystal packing. Such effects can only be taken into account in the calculation by describing at least the first coordination sphere of the molecular environment. Necessarily for TPP this demands huge system sizes which can only be treated by changing to semiempirical or force-field methods. In our tests both methods fundamentally failed to reproduce the crystalline structures c1 and c2. In the case of force-field methods this general disadvantage might be overcome by using self-made potentials adopted to TPP. However, for the purpose presented herein of creating model structures for a conformational analysis the treatment of a single molecule in good quality is sufficient as will be shown later on.

In Table 1 the energies of minima I to VIII are presented relative to structure I. The energies are spread over a range of 9.2 kJ mol^{-1} for both basis sets. Conformer IV is lowest in energy whereas structure V results the highest energies.

Table 1. B3LYP minimum energies for TPP conformers; all values are given in kJ mol^{-1} and refer to the energy of structure I.

	6-31G(d)	6-31+G(d,p)
I	0.0	0.0
II	−0.9	−1.4
III	−1.4	−1.3
IV	−1.7	−1.8
V	7.2	7.4
VI	(to IV)	−0.9
VII	7.5	(to VIII)
VIII	3.5	2.6

Conformer I corresponds to the thermodynamically stable polymorph c1. It is energetically less favorable than four other structures (II, III, IV and VI) which narrowly distribute in a range of 1 kJ mol^{-1}. At a closer look the conformational arrangement in the gas phase seem to result from an interplay between the requirement to minimize sterical hindrance on the one hand and the formation of six-ring arrangements with intramolecular hydrogen bonds on the other hand (see Figure 2). Structure I exhibits no hydrogen bonds and results exclusively from the minimization of sterical hindrance. All minima lower in energy are stabilized by one or two intramolecular hydrogen-bond formations.

For the overall conformational distribution the range of the minimum energies is only small. This means that in the liquid state all of the energetically favored structures should be found as is later on proven through the comparison of 1D ^{31}P spectra. Also for the solid state no unambiguous preferential conformer can be extracted. As a consequence any observed preference of a conformational arrangement in phase aII should be caused by interactions with the surrounding environment, namely the formation of small clusters of TPP molecules.

Ab initio CSA tensors: In addition to the structures Figure 2 shows ab initio calculated NMR tensors for the labeled TPP sites (see also Figure 1). The ellipsoids represent the traceless symmetric part of the second rank tensor which is characterized via the asymmetry parameter η and the coupling constant δ. The orientation of the ^{13}C tensor with respect to the corresponding phenyl moiety is nearly identical in all

 © 2007 Wiley-VCH Verlag GmbH & Co. KGaA, Weinheim

structures. The z axis points along the CO bond with only small aberrations ($\lesssim \pm 5°$) caused by a variation of the local electronic environment due to conformational changes. The x axis appears to be perpendicular to the phenyl plane. With this fixed alignment of the tensors the ^{13}C spin diffusion spectra can be directly interpreted in terms of the structural arrangement of phenyl groups.

The isotropic shift (σ_{iso}) as well as the anisotropy (δ) and asymmetry (η) parameters were extracted for the labeled sites in all single molecule model structures. δ varies in the narrow range of 83.5–89.9 ppm for the CO carbon atoms C1, C2 and C3. Due to this insensitivity towards structural changes this parameter is not suited for a distinction between conformers in the system investigated herein and thus is not taken into account for the following discussion.

Table 2 lists the ab initio values for σ_{iso} and η. C1, C2 and C3 denote the labeled carbon sites in the left, middle and right phenyl ring as shown in Figure 2. Because the calculated data is not referenced, only the relative shifts and the maximum difference $\Delta\sigma_{iso}$ are discussed. It can nicely be seen that the chemical shift gives a direct measure of the molecular symmetry (I and VIII in Table 2). Structure I exhibits C_s symmetry and thereby has two distinguishable signals. The C_3 symmetric structure VIII shows only one isotropic NMR signal. For structure III the above-mentioned broken C_s symmetry is revealed. Even though only slightly different three isotropic shifts can be found for the labeled sites. The relative isotropic shift ranges from 0.00–6.03 ppm with a maximum splitting of 0.00–4.56 ppm for the particular conformer. The asymmetry parameter η ranges from 0.63 to 0.96 with differences of up to 0.33 for the particular conformer.

Table 2. σ_{iso} and η values calculated with B3P86/cc-pVDZ (for definitions and conventions see Figure 2 and Experimental Section); additionally the maximum difference is given as $\Delta\chi = \chi_{max} - \chi_{min}$.

σ_{iso}/ppm	C1	C2	C3	$\Delta\sigma_{iso}$
c1^{DFT}	4.56	0.00	4.39	4.56
I	4.10	0.09	4.10	4.01
II	3.42	0.78	1.59	2.64
III	3.06	3.14	3.00	0.14
IV	3.08	3.41	3.70	0.62
V	6.03	3.34	3.76	2.69
VI	3.32	2.99	3.79	0.80
VII	3.29	3.02	1.05	2.24
VIII	3.40	3.40	3.40	0.00
η	C1	C2	C3	$\Delta\eta$
c1^{DFT}	0.96	0.63	0.94	0.33
I	0.91	0.63	0.91	0.28
II	0.92	0.63	0.75	0.29
III	0.84	0.78	0.84	0.06
IV	0.87	0.73	0.84	0.14
V	0.75	0.76	0.93	0.18
VI	0.90	0.73	0.84	0.17
VII	0.87	0.86	0.74	0.13
VIII	0.85	0.85	0.85	0.00

From that in principle a conformational analysis of TPP is feasible through the comparison of the ab initio values with experimental data obtained at an adequate resolution (0.2–0.3 ppm as found in the MAS spectra of the crystalline phase c1). Unfortunately experimental difficulties restrict the use of MAS to c1. Only wide-line spectra can be recorded for all three TPP phases. Due to the intrinsically lower resolution in these spectra it is questionable whether the calculated differences in $\Delta\sigma_{iso}$, δ and η still allow for a conformational analysis on the base of the ^{13}C nucleus.

Another possibility is to use ^{31}P wide-line spectra. Table 3 lists the ab initio NMR parameters for the phosphorus nucleus in the respective minimum structures. The isotropic shift varies in a range of about −22 up to 25 ppm with respect to structure c1^{DFT}. Furthermore the anisotropy changes up to 22% and η varies from 0.0 to 0.3 (for a comparison, δ changes up to 8% at the carbon nuclei). These major changes allow for at least a qualitative conformational analysis even with low-resolution wide-line spectra. Exemplarily Figure 3 shows ^{31}P spectra which match best with the experimental data for aI, aII and c1 published in the literature.[43] In the simulation phase aI consists of structures I-IV and VI–-VIII. Conformer V had to be excluded from the distribution of the glass. This is a particularly interesting fact since this conformer is found to be amongst the structures highest in energy. The simulation of phase aII bases on structures I and III, thereby significantly narrowing the conformational distribution. Finally c1 is exclusively represented by structure I. This overall situation matches the stepwise narrowing of a conformational distribution as proposed in the Section on Triphenylphosphite and in the literature.[43] However, no detailed picture of the phenyl moieties can be drawn from ^{31}P spectroscopy alone. For example it would not be possible to differentiate between minima III and IV even though these two exhibit pronounced structural differences (see Figure 2 and Table 3 for comparison). Therefore the following discussion exclusively deals with the ^{13}C nucleus.

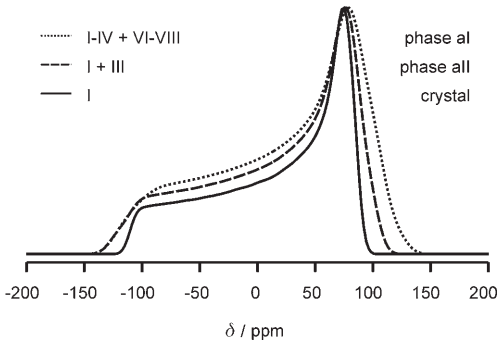

Figure 3. Theoretical simulation of ^{31}P spectra for different conformational distributions in aI, aII and c1 (to account for a glassy state the spectra for aI and aII were treated with an additional Gaussian broadening); the picture matches very well with experimental spectra published by Senker et al.[43]

 © 2007 Wiley-VCH Verlag GmbH & Co. KGaA, Weinheim

Table 3. Ab initio parameters for ^{31}P calculated with B3P86/cc-pvdz; σ_{iso} and δ are given in ppm; σ_{iso} is given as a relative shift with respect to structure $c1^{DFT}$.

	σ_{iso}	δ	η
$c1^{DFT}$	0.0	−120.1	0.13
I	−4.1	−127.0	0.10
II	−7.1	−132.4	0.07
III	−1.7	−146.7	0.15
IV	−3.3	−145.3	0.09
V	−22.1	−131.9	0.21
VI	0.3	−142.3	0.11
VII	25.4	−138.8	0.17
VIII	15.6	−140.8	0.00

1D ^{13}C NMR spectra: Figure 4a shows the experimental MAS spectra of phase c1 recorded for a spinning frequency of 3 kHz. Three separated signals with maximum splitting of 5.05 ppm can be observed. The emersion of these three signals in the experiment accounts for the broken C_s symmetry due to packing effects in the crystal.[40,44] Furthermore Table 4 shows the ab initio calculated values of conformer

Table 4. Comparison of the ab initio and experimental anisotropy of c1.

	C1	C2	C3	C1	C2	C3
		δ/ppm			η	
$c1^{DFT}$	83.5	89.9	84.3	0.96	0.63	0.94
FIT	92.3	93.1	86.7	0.79	0.47	0.79

$c1^{DFT}$ together with the results of a fit using three isolated one spin systems. Upon comparison it is evident that no major differences occur, neither for δ nor for η. The ab initio parameters are ratified by the fit in their order of magnitude. Although the absolute ab initio values of η are overestimated by 0.16 compared with the experiment the relative trend for C1, C2 and C3 is well reproduced. This systematic deviation leads to the result that the difference in η can be taken as a measure in addition to the chemical shift in a conformational analysis.

In comparison with the structures I–VIII only I shows a similar wide splitting of the chemical shift (see Table 2). Structure I represents the gas phase minimum structure of polymorph c1. In comparison with the ab initio values of $c1^{DFT}$ an assignment of the signals is possible. According to the definition used above the carbon atoms C1, C2 and C3 exhibit chemical shift values of 153.3, 148.3, and 152.5 ppm, respectively.

Figure 4b shows one-dimensional wide-line ^{13}C spectra for the phases aI, aII and the crystalline phase c1. For the phases aI and aII no difference in the spectral shape is observed. Only in the crystalline phase the different chemical shifts are resolved and lead to a characteristic form of the spectrum. The general difference between the crystalline and glassy phases can nicely be modeled with the use of the ab initio calculated tensors. The crystalline phase has been simulated using structure I as a model. The glassy states of aI and aII are represented by a superposition of simulated

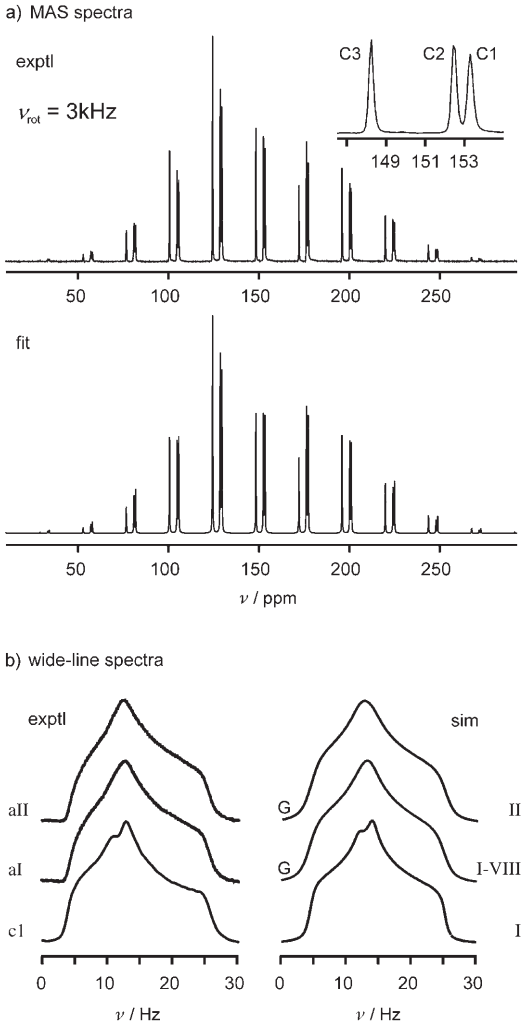

Figure 4. a) MAS spectrum of phase c1 and result of a fit taking the ab initio calculated anisotropy parameters of $c1^{DFT}$ as initial values. b) Measured and ab initio simulated wide-line 1D spectra of the phases aI, aII and c1; for the simulation of a glassy state an additional Gaussian broadening (G) was applied to account for a broad conformational distribution.

spectra for the structures I–VIII. To account for the even broader conformational distribution in a glass a Gaussian line-broadening has been applied. In addition to these models a simulation of the glassy state based exclusively on conformer II has been tried. Even though this would be an unlikely model the qualitative difference between the crystalline and glassy states still is reproduced reasonably well. From these results it is obvious that wide-line 1D spectroscopy is not suited to extract structural details of phase aII. Therefore we additionally performed wide-line 2D rf-driven spin-diffusion measurements.

2D correlation spectroscopy: Spin-diffusion exchange spectroscopy includes the chemical shift parameters σ_{iso}, δ and η as well as the orientation of neighboring tensors towards each other. In a fixed spatial arrangement the orientation correlation causes characteristic ridges in the 2D exchange

 © 2007 Wiley-VCH Verlag GmbH & Co. KGaA, Weinheim

experiment.[39] The spin-diffusion range and with that the number of interacting spins can be controlled by the mixing time t_m. During t_m the spin-diffusion spreads into space and leads to off-diagonal ridges for all spins which participate in the exchange. An exception are parallel tensors where the respective signal remains on the diagonal of the spectrum. All spins which did not take part in the exchange appear on the diagonal as well. A more detailed explanation of the method is given in the literature.[39]

For $t_m \rightarrow \infty$ the spectra can be interpreted as a superposition of ridges for all tensor arrangements found in a sample. Due to experimental reasons t_m is limited to a few hundred milliseconds, which is, however, sufficient to reflect a structural picture of the investigated phase on a mesoscopic scale. The observed pattern is much like a fingerprint of the structural environment and highly sensitive to changes in the spatial arrangement. In the case of TPP with the already discussed fixed ^{13}C tensor orientation for the phenyl groups (see section on ab initio CSA tensors) it directly reflects the structural arrangement of the molecules and has a strong potential for an analysis of conformational arrangements even in the disordered phases. TPP spectra were recorded for mixing the times $t_m = 4$, 10 and 40 ms. As it is not likely that isolated spin pairs occur in the TPP phases it can be assumed that the polarization transfer is homogeneous with t_m. As a consequence the off-diagonal part of the 2D spectra can be analyzed in terms of an orientation correlation even for finite t_m and the diagonal part can be neglected.

Figure 5 shows measurements of phases aI, aII and c1 for the three different mixing times. For the crystalline phase c1 the characteristic pattern exhibits two strongly pronounced wings that are connected through a bridge perpendicular to the diagonal of the spectrum. In addition to that two extensions in the off-diagonal corners of the spectrum can be found. These features are observed for all three mixing times. For $t_m = 4$ ms only the most intense features remain clearly visible. Turning to the structural glass aI the characteristic pattern is much different. Here the spectrum shows two straight features which are perpendicular to each other and include an angle of 45° with the diagonal. Again they remain visible for all three mixing times. By comparison of $t_m = 4$, 10 and 40 ms for the respective spectra of c1 and aI it can be stated that our assumption of a homogeneous polarization build-up is justified. No major changes in the spectral patterns are observed.

Starting with the smallest mixing time 4 ms it can be seen that phase aII neither exactly exhibits the pattern found for aI nor the pattern for the crystal. The most emphasized feature is a broad bridge perpendicular to the diagonal. In addition to that wing-like structures similar to the crystalline pattern are found. This similarity to the ordered state c1 becomes more obvious when comparing the spectra for $t_m =$ 10 ms. Again the broad bridge is found for phase aII. Apart from that all features of the crystalline phase are observed as well clearly demonstrating an ordered state similar to c1. For the largest mixing time 40 ms the c1 features are completely obliterated. The spectrum is highly similar to the

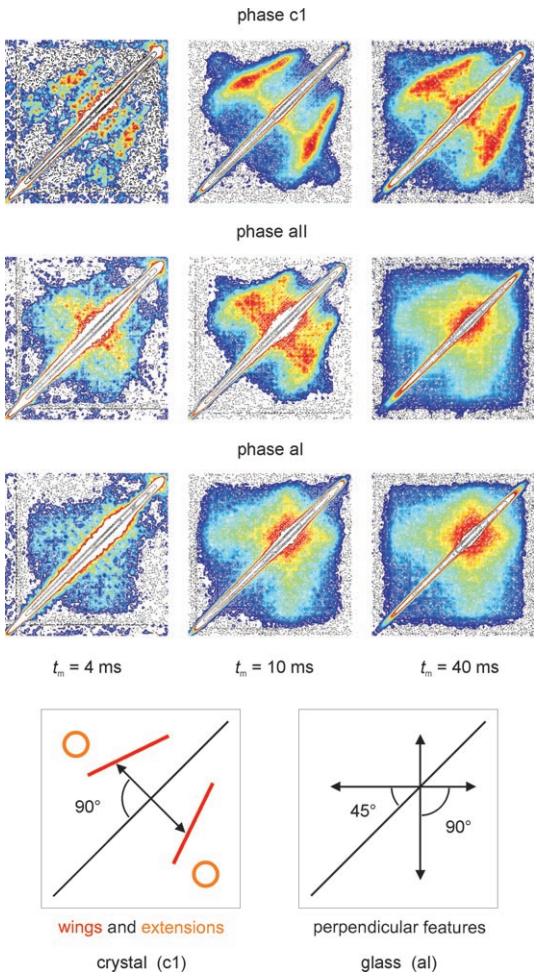

Figure 5. 2D spectra showing the tensorial orientation correlation in the phases aI, aII and c1; for phases aI and c1 the typical features of the ordered and disordered state are sketched.

measurement of phase aI with only minor differences resulting from the underlying crystal-like features. This reflects an amorphous structure of aII as described in the literature.[39]

In general the relationship between the mixing time t_m and the observed spin-diffusion range cannot be expressed analytically, especially not for the disordered phases aI and aII.[39] Nevertheless we can use the mixing time for a qualitative understanding of the structural features of aII by comparing the spectral changes in aI, aII and c1 with t_m. In an intramolecular range (4 and 10 ms) a broad conformational distribution is found for phase aI. After the conversion to phase aII this distribution is significantly narrowed and the spectrum becomes similar to the crystalline phase c1 where only one conformer is present. For an intermolecular range (40 ms) phase aII shows disorder as its dominant structural feature. Even though the measurements clearly reveal different conformational distributions in the TPP phases the description still lacks the explanation on a molecular level. For a more detailed understanding of the observed spin system we carried out simulations of the 2D exchange spectra.

© 2007 Wiley-VCH Verlag GmbH & Co. KGaA, Weinheim

Simulations of 2D exchange spectra: Before turning to a detailed conformational analysis of the 2D spectra we simulated a spectrum for the glassy state. This can be done by a two-dimensional convolution of a wide-line 1D spectrum.[39] Figure 6 (glass) shows such a 2D spectrum created from the 1D ab initio spectrum (I–VIII) presented in Figure 4. In comparison with Figure 5 the simulation nicely matches the measurements of phases aI and aII with $t_m = 40$ ms. Therefore the description of these phases as orientationally disordered states is justified for long exchange ranges. Other than in aII this statement still holds for $t_m = 4$ and 10 ms in phase aI. Thus the molecules in aI are not only randomly oriented towards each other but also show a broad conformational distribution exactly as expected from the common picture of a structural glass. Furthermore, Figure 6 presents

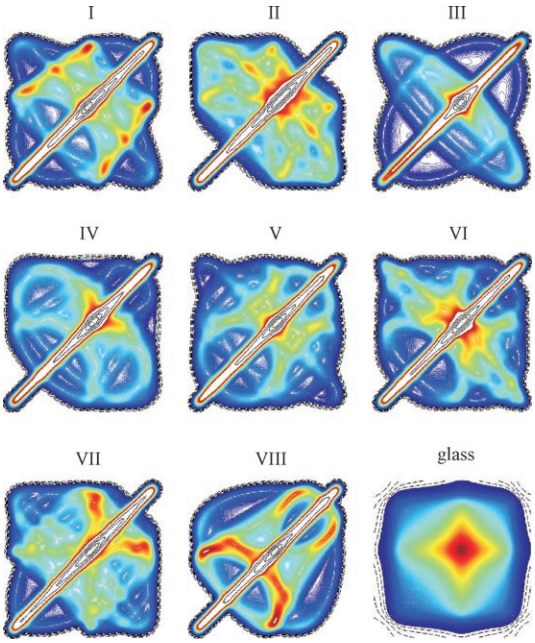

Figure 6. Simulations ($t_m \rightarrow \infty$) of 2D exchange spectra for the model structures I–VIII (see Figure 2) and the glassy state.

the 2D exchange spectra for the structures I–VIII. All eight conformers exhibit a unique spectral pattern characteristic for the particular conformation. This clearly demonstrates the prediction power of orientation correlation spectroscopy for conformational analyses. In comparison with the measurements the simulation for minimum structure I matches the spectra of the crystalline phase c1 best. It is the only case where pronounced and well separated wing structures are found. In addition to the wings the typical extensions observed for c1 occur as well. The interconnecting bridge between the wings is not well represented in the simulation. Another difference is found in the intensity distribution over the wings. These differences can of course originate in the comparison of a simulation for $t_m \rightarrow \infty$ with a spectrum measured for at a finite mixing time. However, if the assumption of a homogeneous polarization transfer is valid it is more likely that the observed features result from a conformational distortion of the ideal gas-phase structure I. In Figure 7 the simulation for conformer $c1^{DFT}$ is shown together with the measurement of c1 for $t_m = 40$ ms. In comparison

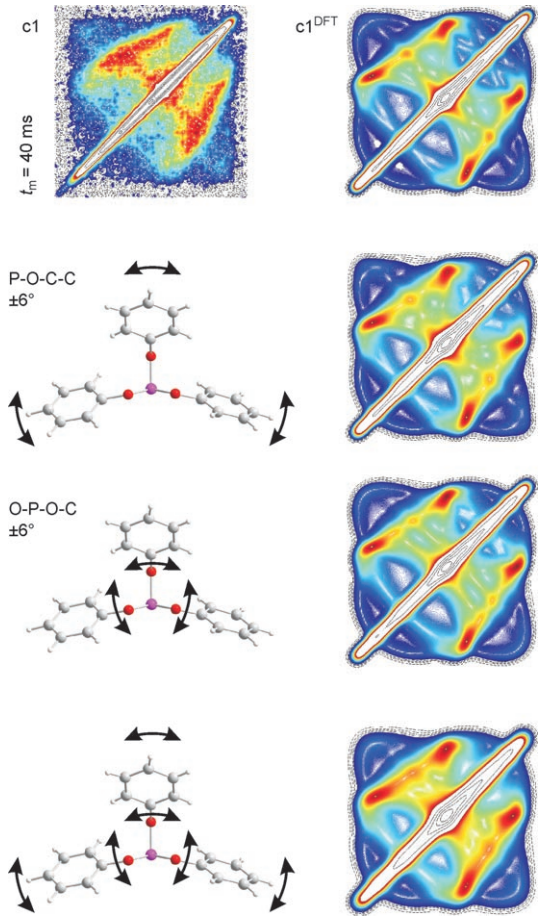

Figure 7. Simulations ($t_m \rightarrow \infty$) and experiment for phase c1; the influence of small variations of the phenyl orientation on the spectral shape is shown.

to the simulation of structure I (see Figure 6) the spectrum of $c1^{DFT}$ resembles the measurements in much more detail. In particular close to the diagonal a bridge-like feature 90° with respect to the diagonal appears. In addition to that the overall shape of the wings is closer to that found in the experiment. To test the relation between the chemical shift principle values and the spectral shape a second simulation has been carried out using the σ_{iso}, δ and η of the experimental fit together with the tensorial orientations of $c1^{DFT}$. It turned out that small changes in these parameters do not have any pronounced influence on the spectrum. With this the orientation of the tensors in the system is the dominant and important variable for the simulations. The clearly different 2D spectra of I (see Figure 6) and $c1^{DFT}$ (see Figure 7) demonstrate the extreme sensitivity of the spectral shape towards minor structural changes. To investigate the importance of such changes for the spectrum of the crystalline phase further model structures have been calculated to-

 © 2007 Wiley-VCH Verlag GmbH & Co. KGaA, Weinheim

gether with their 2D spectra. For all three phenyl groups a stochastic distribution of the P-O-C-C and O-P-O-C dihedrals has been assumed and the angles varied in seven steps from −6 to +6° with respect to the orientation in C1^{DFT}. Because only small changes were applied the structural relaxation of the molecule was neglected and the models calculated as single points. The resulting 343 NMR spectra have been added up for the respective dihedral angle and the results are shown in Figure 7. The variation of the P-O-C-C angles leads to an overall broadening of the pattern observed for c1^{DFT}. In contrary to that the variation of O-P-O-C does not alter the shape of the wings. The spectral pattern remains sharp and two bridges form between the diagonal and the wings. Close to the diagonal the intensity distribution changes its pattern compared to the simulation for c1^{DFT}.

Changes about dihedral angles of ±6° are well in agreement with the atomic displacement parameters found for the crystal structure of c1.[40] Thus even for the crystalline phase one can expect that the 2D spectrum results from an ensemble of molecules with small structural deviations from a mean arrangement which is represented by structure c1^{DFT}. It should be noted that whereas librational dynamics leads to a partial averaging of the CSA tensor (which is expected to be small at 190 K) the here observed differences in the spectral shape clearly account for a structural distribution representing static disorder in the crystalline phase. To test the overall influence of such a distribution both spectra for variations about P-O-C-C and O-P-O-C were added up and a small additional Gauss broadening was applied. This broadening is meant to account for effects caused by the much higher degree of freedom of the molecule than included in our model system. The result is very close to the experimentally observed spectrum (see Figure 7). Therefore it can be stated that for the simulation of the details of the measurements it is necessary to take into account an ensemble of representative model structures. Because of the high sensitivity to changes in tensorial orientations these structures were generated via a small and stepwise distortion from a proposed mean structure. Through this procedure an analysis of the tensorial orientation within an accuracy of about 10–20° should be possible when large changes in the 2D spectrum are involved.

In a next step a detailed analysis of phase aII was carried out. In particular aII differs from the crystalline phase c1 through the emersion of a pronounced broad bridge in the spectrum for $t_m = 10$ ms (see Figure 5). As seen above such a feature cannot result from small angle deviations. Therefore we generated further model structures for large angle deviations and simulated the respective 2D spectra. For these large variations the structural relaxation of the overall molecule cannot be neglected anymore. Consequently we started our analysis from minimum structure I and gradually created new structures through scans of single dihedral angles as described for the conformational search (see Experimental Section). For symmetry reasons only rotations of the C1 and C2 phenyl rings have to be considered (see Figure 8). First

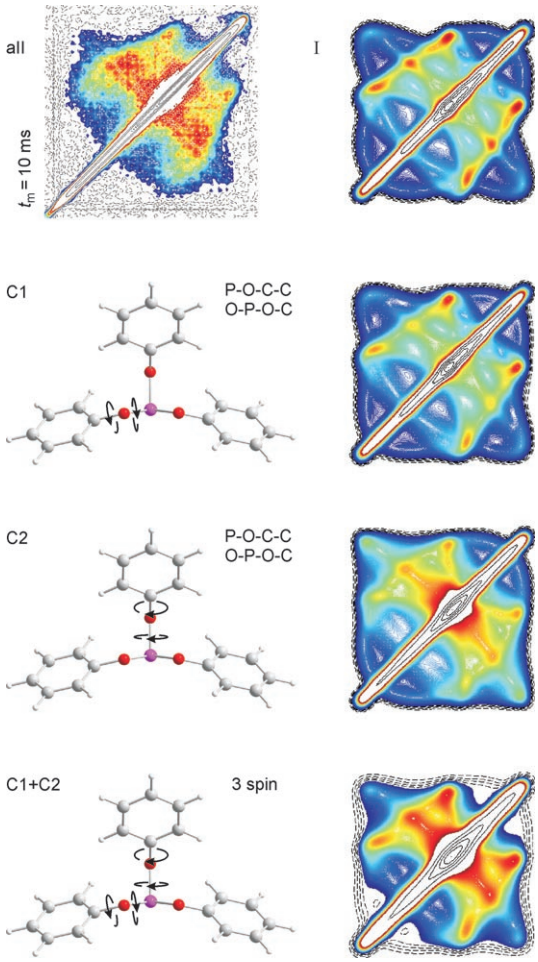

Figure 8. Simulations ($t_m \rightarrow \infty$) and experiment for phase aII demonstrating the influence of large variations in dihedral angles on the spectra for three-spin systems.

the P-O-C-C and O-P-O-C dihedral angles were varied for both rings, then the resulting NMR spectra were added up. Representative results of these investigations are shown in Figure 8. For C1 the scans of P-O-C-C and O-P-O-C were carried out from −14 to 18° and −16 to 43°, respectively. C2 variations ranged from 0 to 39° for P-O-C-C to 0 to 55° for O-P-O-C. The change in C1 appears to have a minor effect on the spectral shape. Compared with the simulation for structure I the overall shape remains the same whereas the intensity distribution along the wings changes. When turning to C2 drastic changes appear in the spectrum. The wing structure is broken up and a broad bridge about 90° with respect to the diagonal arises. This feature fits very well with the experimentally observed bridge. Model systems with structural changes different from the above described procedure have been tried as well but in no case similar features could be found. Furthermore structure I is the only possible choice for a mean structure because all other conformers exhibit strongly diverse spectral patterns (see Figure 6) which do not reproduce the characteristic wings. Thus the distortion of C2 starting from structure I is the most reasonable explanation for the observed 2D spectra of phase aII. This

 © 2007 Wiley-VCH Verlag GmbH & Co. KGaA, Weinheim

means that in phase aII a preferential conformer exists which resembles the mean structure I and exhibits a disorder of the phenyl groups in a minor range of the dihedral distortions.

In the overall simulation of phase aII all angular displacements should be represented. Therefore we added up the 2D spectra for C1 and C2. As in the crystalline simulation a small Gaussian broadening has been applied for effects not included in our model. The result is shown in Figure 8 ("C1 + C2"). It nicely reproduces all important spectral features found in the experimental spectrum of phase aII. Even though only this one example is presented in this work other variations of the dihedral angles of C2 have been tried with similar success. It turned out that for the given distortion of the C1 phenyl ring C2 can be varied in a range up to 39–49° for P-O-C-C and 45–65° for O-P-O-C. With that the disorder of the C2 phenyl ring is described very precisely. This is an even more exciting result when considering that this analysis has been carried out for a locally ordered structure in an amorphous phase. Unfortunately changes in the orientation of C1 do not exert a strong influence on the spectrum which is why such a detailed analysis is limited to the middle phenyl ring of structure I.

2D exchange spectra of larger spin systems: A basic assumption in the preceding discussion is that at $t_m = 10$ ms only spectral features resulting from a single TPP molecule are visible. To verify this hypothesis we increased our model to a system containing two TPP molecules, the largest system that could be treated reasonably well with ab initio methods. A TPP pair was cut out from the crystal structure of c1 where the TPP molecules are found to be aligned in parallel.[40,44] This arrangement was taken as a starting structure and optimized further with different methods and basis sets.

With the HF method two different minima could be found which exhibit a strong distortion of the molecules towards each other. This manifests in strongly diverse OH distances and a PP distance which is about 30% longer compared with one in the crystal structure (see Table 5). Changing to the B3LYP functional the molecules tend more towards a parallel orientation, which leads to a smaller PP distance whereas the large value for OH3 still indicates a distortion of the molecules. This changes with the introduction of the PBE1PBE functional. For three different basis sets the mean aberration of the PP distance is only about 3%. The OH distance deviations improve to ≤ 10% with increasing the basis set.

Table 5. Distances and pair-formation energies (minimum and MP2/6-31G(d)) for structures described in Figure 9; all energies have been counterpoise corrected for BSSE[46] and are given in kJ mol^{-1}; distances are given in Å.

	OH1	OH2	OH3	PP	E^{MIN}	E^{MP2}
X-ray	2.99	3.52	2.95	5.72	–	–
1)[a,d]	2.83	3.51	3.50	7.22	−3.3	−21.8
2)[a,d]	2.97	2.88	3.09	7.55	−3.9	−21.5
3)[b,d]	2.60	2.97	4.33	6.39	1.7	−23.3
4)[c,d]	2.72	3.07	3.53	5.90	−5.0	−26.4
5)[c,e]	2.98	3.31	3.30	6.00	−8.2	−25.4
6)[e,f]	3.04	3.33	3.26	5.85	−7.7	−26.3

[a] HF. [b] B3LYP. [c] PBE1PBE. [d] 6-31G(d). [e] 6-31+G(d,p). [f] 6-311++G(d,p).

Table 5 as well lists counterpoise corrected pair-formation energies for the above described structures. Because significant amounts of the dispersion energy are neglected by HF and DFT in addition the results of MP2 calculations are shown. With MP2 all structures pose stable minima with reasonable stabilization energies that match the values that could be expected for a dimer with three weak OH contacts.[45] Even though it cannot be claimed that any of the structures represents a minimum on the MP2 surface, a stability order can be established for the TPP pairs. In comparison with the structural data in Figure 9 it can be seen that

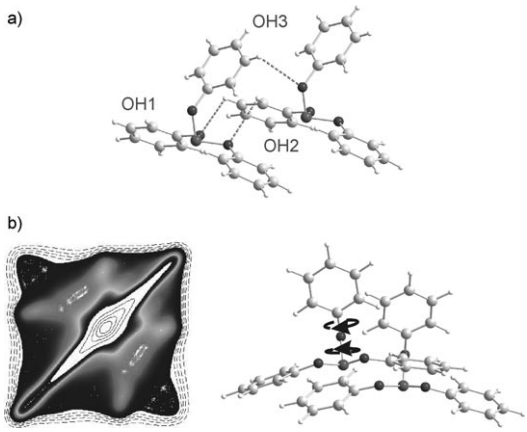

Figure 9. a) Definition of chosen OH contacts for the methodological comparison in Table 5. b) Simulation ($t_m \rightarrow \infty$) of the influence of large variations in dihedral angles for 2D spectra of six-spin systems.

the MP2 energies correlate with the PP distance. The lowest PP distances yield a maximum stabilization of the system (about -26 kJ mol^{-1}). With about -22 kJ mol^{-1} the strongly distorted HF structures give the smallest stabilization energies. Because the PP distance not only correlates with the stabilization energy but also is an indicator for the parallel alignment of the TPP molecules it can be concluded that a parallel arrangement leads to energetically favored structures.

We furthermore repeated the distortional variation of C2 for a TPP pair (see Figure 9b) and calculated the NMR spectrum as a six-spin system. It can be seen that the characteristic bridge completely vanished from the spectrum (compare to Figure 8). The six-spin simulation of C2 differs significantly from the corresponding three-spin system. Consequently, for $t_m = 10$ ms intramolecular arrangements dominate the exchange spectra which can be interpreted in terms of a conformational analysis as it was done above. At a closer look the intensity distribution in the most outstanding region of the six-spin simulation near the diagonal resembles the experiment better than in the three-spin case. Thus it might be that to some percentage the first coordination

 © 2007 Wiley-VCH Verlag GmbH & Co. KGaA, Weinheim

sphere is also visible. However, this is only a minor effect and it does not affect the overall interpretation.

These results are of immediate importance for the project of a direct determination of TPP clusters in phase aII. This can be accomplished using the concerted approach described herein. Whereas in the paper at hand we focused on the intramolecular correlation of ^{13}C tensors our current project deals with the separation of intra- and intermolecular exchange. For this the mixing time t_m has to be increased to values above 10 ms. Additionally such measurements can not be performed with triply [^{13}C]-labeled TPP anymore. In such a sample the overlap of intra- and intermolecular interactions completely destructs the necessary sensitivity of the spectral pattern towards structural features (see Figure 9). However, this overlap can be avoided using monolabeled 1-[^{13}C]-TPP. Due to the omnipresent transesterification of mixed aryl phosphites at room temperature and above the preparation of this system affords the development of a low-temperature synthesis. Furthermore, at the computational edge of the approach systems containing a several TPP molecules have to be treated for reasonable structure models. This is only possible by using force field methods which are manually adapted to the TPP system. All this work is currently in progress in our group and will be published in a forthcoming paper.

Conclusions

Our concerted approach including synthesis, computational chemistry and solid-state NMR spectroscopy for structural investigations was successfully applied to unravel the distribution of conformers in one ordered (c1) and two disordered phases (aI and aII) of triphenylphosphite.

In a conformational analysis based on DFT eight different minimum structures were identified for TPP, two of them representing the conformations of the crystalline phases c1 and c2. Apart from distortions caused by crystal packing the gas-phase calculations match the experimental structures surprisingly well. The energies show that none of the structures is unambiguously favored over the others. The structures served as a base for the ab initio calculation of the chemical shift tensors and a subsequent simulation of NMR experiments.

For a sample of tri-(1-[^{13}C]phenyl)-phosphite a variety of 1D MAS and wide-line spectra were measured and their potential for a conformational analysis in the different TPP phases were investigated. In the case of the crystalline phase c1 MAS experiments are well suited for a conformational analysis. The comparison of the chemical shift values σ_{iso} and η with their ab initio counterparts allow for an unequivocal assignment. However, the 1D ^{13}C wide-line spectra do not allow to distinguish between different conformational distributions.

Furthermore all of the TPP phases were investigated by 2D rf-driven spin-diffusion spectroscopy. With this method a detailed picture of aI, aII and c1 could be achieved. On a larger length scale aI and aII appear as disordered phases whereas c1 is clearly crystalline and exhibits a well defined long range order. The intramolecular arrangement differs significantly in all the three phases. Phase c1 exhibits only one conformation as expected for a crystalline phase. In aI a broad distribution of conformations is observed, consistent with the picture of a structural glass. Phase aII, however, consists of a mean preferential conformer similar to that in phase c1. Nevertheless, in contrary to c1 a significant conformational distribution is still present. By comparison with simulations this distribution could be attributed to the middle phenyl ring which is distorted in the narrow range of 10–20° about two dihedral angles.

We could show that the use of the concerted approach in combination with 2D exchange spectroscopy has a strong potential for the investigation of the local order in disordered materials. The approach is highly adjustable to the individual problem. Therefore it is well suited for the investigation of similar structural problems as there exist many. Self-assembly studies in highly disordered environments should become accessible like the investigation of the aggregation of nucleating agents in polypropylene.[47] Another great area of application is for biological systems. Here the disruption of lipid bilayer membranes by antimicrobial peptides is a good example for examination.[48] Finally trendsetting research topics like nucleation and growth or nanoscopic self-assembly have a high demand for innovative analytical methods as on the here important length scale classical methods like X-ray diffraction fail to reveal the important structural details.[1–5,49]

Experimental Section

Synthesis: The wide-line NMR experiments presented in this work demand a sufficient amount of tri-(1-[^{13}C]phenyl)-phosphite which can be synthesized from PCl_3 and 1-[^{13}C]phenol.[50] The products have been confirmed using liquid ^1H, ^{13}C and ^{31}P NMR performed on a JEOL Eclipse 400 spectrometer. Enrichment and purity of the 1-[^{13}C]phenol was determined by GC/MS on a Agilent HP 6890/MSD 5973 apparatus.

We decided to prepare monolabeled phenol from sodium 1-[^{13}C]acetate (EURISOTOP, 99% ^{13}C), following the seven-step synthesis of Rieker et al.[51] An overall yield of 70% 1-[^{13}C]phenol with respect to the educt could be gained (lit.: 67%). No traces of impurities could be found in ^1H NMR and GC/MS measurements. The degree of isotope enrichment could be determined to 97% from mass spectrometry results.

The high purity of educts is the essential factor in the following synthesis of tri-(1-[^{13}C]phenyl)-phosphite from PCl_3 and 1-[^{13}C]phenol. Freshly received PCl_3 (Merck, 99%) was distilled twice (b.p. 72°C) and stored in dry flasks under argon. To prevent oxidation the synthesis as well was carried out under argon atmosphere. 1 equiv PCl_3 were added dropwise to 3.5 equiv 1-[^{13}C]phenol over 45 minutes. In the beginning of the reaction the development of HCl and cooling of the mixture could be noticed. The mixture was heated to 120°C for 2 h until no gas production could be observed anymore. The surplus of phenol was then removed through vacuum distillation at 120–125°C and 1×10^{-3} mbar. This procedure yielded a residue of colorless tri-(1-[^{13}C]phenyl)-phosphite (99% with respect to PCl_3). Solution ^1H and ^{31}P NMR determined the purity of the sample to 100%.

Solid-state NMR measurements: ^{13}C NMR measurements were performed on a conventional DSX Avance spectrometer (Bruker, Germany)

 © 2007 Wiley-VCH Verlag GmbH & Co. KGaA, Weinheim

operating at a ^{1}H frequency of 500 MHz. For MAS and wide-line experiments the crystalline phase c1 was prepared at 250 K from the supercooled liquid outside the spectrometer. In contrary phases aI and aII were directly prepared inside the spectrometer using the procedures described by Senker et al.[39] 213 K has been chosen as annealing temperature for phase aII. The temperature was adjusted via a constant flow of cold, dry nitrogen with an accuracy of ± 2 K. Static samples were degassed using the pump and freeze technique and sealed off under vacuum. Liquid NMR measurements showed that the main impurity in these samples was less than 3% triphenylphosphate.

1D MAS spectra were recorded at 200 K with a commercial 4 mm MAS probe (Bruker) and referenced to TMS. For data acquisition a ramped cross-polarization pulse sequence with a contact time of 5 ms and a 90° pulse length of 3.4 μs was used. During acquisition proton decoupling was achieved with a TPPM pulse sequence.[39]

Samples for wide-line experiments were mounted in a commercial CP double resonance probe (Bruker) equipped with a 5 mm solenoid coil. All measurements were carried out at 190 K to eliminate all relaxation processes of supercooled liquids and to reduce an averaging of the CSA interaction by librational dynamics.[52] 1D spectra were recorded with a Hahn-echo pulse sequence where the preceding 90° pulse was replaced by ^{1}H,^{13}C cross polarization (contact time 3 ms). The investigation of the orientation of neighboring molecules was carried out using two-dimensional radio-frequency-driven spin-diffusion[53] exchange spectroscopy[38,39] with a WALTZ17 composite spin-lock sequence. 90° Pulse lengths were set to 2.5–3.0 μs, in the composite lock a nutation frequency of 125 kHz was used. For methodological details the reader is referred to the literature.[38,39,53] Continuous wave broadband proton decoupling was applied during the evolution and acquisition periods.

Computational methods: Quantum chemical calculations were performed with the Gaussian03[54] package on ordinary linux clusters. Resources ranged from 32 bit systems with one or two Pentium4 (3 GHz) processors to 64 bit platforms with four parallel Itanium2 (1.3 GHz) processors and were applied as required by the system size or level of calculation. All investigations were based on polymorph c1 as a starting point (see Figure 2). To find a suitable computational level we tested a broad range of Pople basis sets (from STO-3G to 6-311G) by way of geometry optimization of the c1 crystal molecule with the B3LYP functional. In comparison with the crystal structure 6-31G(d) and 6-31+G(d,p) mirrored the experiment best.

The conformational search was performed via scans of the potential energy surface on a computational level of B3LYP/STO-3G. Three different dihedral angles have been varied in the TPP molecule (two about the PO bonds of the middle and right phenyl ring and one about the OC bond of the middle phenyl ring, see Figure 8 for comparison). For each point of the scan one or a maximum of two dihedral angles were fixed whereas the rest of the molecule was allowed to fully relax. Based on these calculations several single points were chosen and further optimized using the bigger basis sets 6-31G(d) and 6-31+G(d,p). For the NMR tensor calculations an additional model system (referred to as c1^{DFT}) was calculated on the base of the X-ray structure of polymorph c1. The c1 conformer was relaxed with B3LYP/6-31G(d) under the constraint of fixed phenyl orientations. In particular this procedure compensated for the experimentally poorly described H atom positions and thus allowed to calculate ab initio NMR tensors for the experimental structure.

In the TPP system containing two molecules a variety of methods (HF, B3LYP and PBE1PBE) and different basis sets has been tested in geometry optimization. Due to their lack of electron correlation which significantly contributes to the pair formation energy for all minima the MP2 single point energy was calculated. The pair formation energies have been corrected for the basis set superposition error (BSSE) using the counterpoise (CP) correction.[46]

The ab initio ^{13}C NMR tensors were calculated using the GIAO method[9] on the B3P86/cc-pVDZ level of theory. In a benchmark study comparing 102 organic systems it was found that even in combination with small basis sets this functional yields good results for aromatic ^{13}C tensors.[55] The here presented isotropic shifts are not referenced and therefore exclusively discussed in terms of their relative positions. For convenience the values are related to the smallest calculated isotropic shift (C2 carbon atom in structure c1^{DFT}).

Spectra simulations: MAS spectra were simulated with the SIMPSON[56] NMR tool. Simulations of wide-line spectra were carried out using self-written programs based on the GAMMA[57] C++ library considering three- and six-spin systems.

For the use of these programs the full ab initio chemical shift tensor as given by Gaussian 03 had to be converted which was done by a self-developed MATLAB[58] interface. In this script first the symmetric and antisymmetric parts are separated by way of tensor reduction: $\sigma=\sigma^{anti}+\sigma^{sym}$.[59] A following solution of the eigenvalue problem for the symmetric part yield the principle values and vectors in the principle axis system (PAS). The anisotropy and asymmetry parameters δ and η are derived from the symmetric tensor according to the conventions used in SIMPSON ($\sigma_{iso}=\frac{1}{3}(\sigma_{xx}+\sigma_{yy}+\sigma_{zz})$, $\delta_{CS}=\sigma_{zz}-\sigma_{iso}$, $\eta=(\sigma_{yy}-\sigma_{xx})/\delta_{CS}$ with $|\sigma_{zz}-\sigma_{iso}|\geq|\sigma_{xx}-\sigma_{iso}|\geq|\sigma_{yy}-\sigma_{iso}|$).[57] The Euler angles (α, β, γ) are given for the transformation from the principle axis system to a reference axis system which is the internal coordinate system of the Gaussian 03 calculation: $\sigma^{sym}(RAS)=\boldsymbol{R}(\alpha,\beta,\gamma)\cdot\sigma^{sym}(PAS)\cdot\mathbf{R}^{-1}(\alpha,\beta,\gamma)$.[59] The output of calculated values can directly be used with SIMPSON and GAMMA. Beside that an additional output allows the pictorial presentation of the anisotropic part of the tensor with DIAMOND.[60]

Acknowledgements

We would like to thank Denis Golovanov for sharing the crystallographic data of polymorph c2.

[1] C. A. Angell, *J. Non-Cryst. Solids* **1985**, *73*, 1–17.
[2] O. Mishima, H. Stanley, *Nature* **1998**, *396*, 329–335.
[3] M. Jansen, B. Jäschke, T. Jäschke, *Struct. Bonding (Berlin)* **2002**, *101*, 137–191.
[4] D. Kivelson, G. Tarjus, *J. Non-Cryst. Solids* **2002**, *307–310*, 630–636.
[5] J. L. Yarger, G. H. Wolf, *Science* **2004**, *306*, 820–821.
[6] C. M. Carter, D. W. Alderman, J. C. Facelli, D. M. Grant, *J. Am. Chem. Soc.* **1987**, *109*, 2639–2644.
[7] M. H. Sherwood, J. C. Facelli, D. W. Alderman, D. M. Grant, *J. Am. Chem. Soc.* **1991**, *113*, 750–753.
[8] R. J. Iuliucci, C. G. Phung, J. C. Facelli, D. M. Grant, *J. Am. Chem. Soc.* **1996**, *118*, 4880–4888.
[9] K. Wolinski, J. F. Hinton, P. Pulay, *J. Am. Chem. Soc.* **1990**, *112*, 8251–8260.
[10] J. C. Facelli, D. M. Grant, *Nature* **1993**, *365*, 325–327.
[11] R. Salzmann, C. J. Ziegler, N. Godbout, M. T. McMahon, K. S. Suslick, E. Oldfield, *J. Am. Chem. Soc.* **1998**, *120*, 11323–11334.
[12] K. Eichele, R. E. Wasylishen, J. F. Corrigan, N. J. Taylor, A. J. Carty, K. Feindel, G. M. Bernard, *J. Am. Chem. Soc.* **2002**, *124*, 1541–1552.
[13] D. Stueber, D. M. Grant, *J. Am. Chem. Soc.* **2002**, *124*, 10539–10551.
[14] A. Poon, J. Birn, A. Ramamoorthy, *J. Phys. Chem. B* **2004**, *108*, 16577–16585.
[15] J. Birn, A. Poon, Y. Mao, A. Ramamoorthy, *J. Am. Chem. Soc.* **2004**, *126*, 8529–8534.
[16] W. Wang, C. G. Phung, D. W. Alderman, J. Pugmire, D. M. Grant, *J. Am. Chem. Soc.* **1995**, *117*, 11984–11988.
[17] J. Heller, D. D. Laws, M. Tomaselli, D. S. King, D. E. Wemmer, A. Pines, E. Oldfield, *J. Am. Chem. Soc.* **1997**, *119*, 7827–7831.
[18] K. Aimi, A. Yamane, S. Ando, *J. Mol. Struct.* **2002**, *602–603*, 417–428.
[19] D. Colombo, P. Ferraboschi, F. Ronchetti, L. Toma, *Magn. Reson. Chem.* **2002**, *40*, 581–588.
[20] J. K. Harper, J. C. Facelli, D. H. Barich, G. McGeorge, A. E. Mulgrew, D. M. Grant, *J. Am. Chem. Soc.* **2002**, *124*, 10589–10595.
[21] M. J. Potrebowski, X. Assfeld, K. Ganicz, S. Olejniczak, A. Cartier, C. Gardiennet, P. Tekely, *J. Am. Chem. Soc.* **2003**, *125*, 4223–4232.

 © 2007 Wiley-VCH Verlag GmbH & Co. KGaA, Weinheim

[22] A. Zheng, M. Yang, Y. Yue, C. Ye, F. Deng, *Chem. Phys. Lett.* **2004**, *399*, 172–176.
[23] C. Ochsenfeld, S. P. Brown, I. Schnell, J. Gauss, H. W. Spiess, *J. Am. Chem. Soc.* **2001**, *123*, 2597–2606.
[24] C. Benzi, O. Crescenzi, M. Pavone, V. Barone, *Magn. Reson. Chem.* **2004**, *42*, S57–S67.
[25] C. Benzi, M. Cossi, V. Barone, R. Tarroni, C. Zannoni, *J. Phys. Chem. B* **2005**, *109*, 2584–2590.
[26] T. Charpentier, S. Ispas, M. Profeta, F. Mauri, C. J. Pickard, *J. Phys. Chem. B* **2004**, *108*, 4147–4161.
[27] C. Gervais, M. Profeta, V. Lafond, C. Bonhomme, T. Azais, H. Mutin, C. J. Pickard, F. Mauri, F. Babonneau, *Magn. Reson. Chem.* **2004**, *42*, 445–452.
[28] C. Gervais, R. Dupree, K. J. Pike, C. Bonhomme, M. Profeta, C. J. Pickard, F. Mauri, *J. Phys. Chem. A* **2005**, *109*, 6960–6969.
[29] R. K. Harris, S. A. Joyce, C. J. Pickard, S. Cadars, L. Emsley, *Phys. Chem. Chem. Phys.* **2006**, *8*, 137–143.
[30] a) M. Baldus, *Angew. Chem.*, 2006, 118, 1204–1207; b) M. Baldus, *Angew. Chem.* **2006**, *118*, 1204–1207; *Angew. Chem. Int. Ed.* **2006**, *45*, 1186–1188.
[31] J. C. Facelli, A. M. Orendt, Y. J. Jiang, R. J. Pugmire, D. M. Grant, *J. Phys. Chem.* **1996**, *100*, 8268–8272.
[32] O. Walker, P. Mutzenhardt, P. Tekely, D. Canet, *J. Am. Chem. Soc.* **2002**, *124*, 865–873.
[33] H. Kaji, T. Yamada, N. Tsukamoto, F. Horii, *Chem. Phys. Lett.* **2005**, *401*, 246–253.
[34] M. Gee, R. E. Wasylishen, K. Eichele, J. F. Britten, *J. Phys. Chem. A* **2000**, *104*, 4598–4605.
[35] J. R. Brender, D. M. Taylor, A. Ramamoorthy, *J. Am. Chem. Soc.* **2001**, *123*, 914–922.
[36] S. Macholl, F. Börner, G. Buntkowsky, *Z. Phys. Chem. (Muenchen Ger.)* **2003**, *217*, 1473–1505.
[37] S. Wi, H. Sun, E. Oldfield, M. Hong, *J. Am. Chem. Soc.* **2005**, *127*, 6451–6458.
[38] J. Senker, L. Seyfarth, J. Voll, *Solid State Sci.* **2004**, *6*, 1039–1052.
[39] J. Senker, J. Sehnert, S. Correll, *J. Am. Chem. Soc.* **2005**, *127*, 337–349.
[40] J. Senker, J. Lüdecke, *Z. Naturforsch.* **2001**, *56b*, 1089–1099.
[41] D. G. Golovanov, K. A. Lyssenko, M. Y. Antipin, Y. S. Vygodskii, E. I. Lozinskaya, A. S. Shaplov, *CrytEngComm* **2005**, *7*, 465–468.
[42] R. Kurita, H. Tanaka, *Phys. Rev. B* **2006**, *73*, 104202.
[43] J. Senker, E. Rössler, *J. Phys. Chem. B* **2002**, *106*, 7592–7595.
[44] O. Hernandez, A. Hedoux, J. Lefebvre, Y. Guinet, M. Descamps, R. Papoular, O. Masson, *J. Appl. Crystallogr.* **2002**, *35*, 212–219.
[45] T. Steiner, *Angew. Chem.* **2002**, *114*, 50–80; *Angew. Chem. Int. Ed.* **2002**, *41*, 48–76.
[46] F. B. van Duijneveldt, J. G. C. M. van Duijneveldt-van de Rijdt, J. H. van Lenthe, *Chem. Rev.* **1994**, *94*, 1873–1885.
[47] M. Blomenhofer, S. Ganzleben, D. Hanft, H. W. Schmidt, M. Kristiansen, P. Smith, K. Stoll, D. Mäder, K. Hoffmann, *Macromolecules* **2005**, *38*, 3688–3695.
[48] K. A. Henzler Wildman, D.-K. Lee, A. Ramamoorthy, *Biochemistry* **2003**, *42*, 6545–6558.
[49] P. Jonkheijm, P. van der Schoot, P. H. J. Schenning, E. W. Meijer, *Science* **2006**, *313*, 80–83.
[50] B. E. Schwickert, S. R. Kline, H. Zimmermann, K. M. Lantzky, J. L. Yarger, *Phys. Rev. B* **2001**, *64*, 045410/1-6.
[51] A. Rieker, K. Schefler, E. Müller, *J. Liebigs Ann. Chem.* **1963**, *670*, 23–30.
[52] K. J. Hallock, D. K. Lee, A. Ramamoorthy, *J. Chem. Phys.* **2000**, *113*, 11187–11193.
[53] B. H. Meier, *Adv. Magn. Opt. Reson.* **1994**, *18*, 1–116.
[54] Gaussian 03, Revision B.01, M. J. Frisch, G. W. Trucks, H. B. Schlegel, G. E. Scuseria, M. A. Robb, J. R. Cheeseman, J. A. Montgomery Jr., T. Vreven, K. N. Kudin, J. C. Burant, J. M. Millam, S. S. Iyengar, J. Tomasi, V. Barone, B. Mennucci, M. Cossi, G. Scalmani, N. Rega, G. A. Petersson, H. Nakatsuji, M. Hada, M. Ehara, K. Toyota, R. Fukuda, J. Hasegawa, M. Ishida, T. Nakajima, Y. Honda, O. Kitao, H. Nakai, M. Klene, X. Li, J. E. Knox, H. P. Hratchian, J. B. Cross, C. Adamo, J. Jaramillo, R. Gomperts, R. E. Stratmann, O. Yazyev, A. J. Austin, R. Cammi, C. Pomelli, J. W. Ochterski, P. Y. Ayala, K. Morokuma, G. A. Voth, P. Salvador, J. J. Dannenberg, V. G. Zakrzewski, S. Dapprich, A. D. Daniels, M. C. Strain, O. Farkas, D. K. Malick, A. D. Rabuck, K. Raghavachari, J. B. Foresman, J. V. Ortiz, Q. Cui, A. G. Baboul, S. Clifford, J. Cioslowski, B. B. Stefanov, G. Liu, A. Liashenko, P. Piskorz, I. Komaromi, R. L. Martin, D. J. Fox, T. Keith, M. A. Al-Laham, C. Y. Peng, A. Nanayakkara, M. Challacombe, P. M. W. Gill, B. Johnson, W. Chen, M. W. Wong, C. Gonzalez, J. A. Pople, Gaussian, Inc., Wallingford, CT, **2004**..
[55] T. H. Sefzik, D. Turco, J. R. Iuliucci, J. C. Facelli, *J. Phys. Chem. A* **2005**, *109*, 1180–1187.
[56] M. Bak, J. T. Rasmussen, N. C. Nielsen, *J. Magn. Reson.* **2000**, *147*, 296–330.
[57] S. A. Smith, T. O. Levante, B. H. Meier, R. R. Ernst, *J. Magn. Reson.* **1994**, *106a*, 75–105.
[58] MATLAB, The language of technical computing, Math Works Inc., 24 Prime Park Way, Natick, MA 01760-1500, Copyright **1984–2004**.
[59] A. Steigel, H. W. Spiess, Dynamic NMR Spectroscopy, Springer, **1978**.
[60] Scientific Computing World, **2002**, *63*, 19–21.

Received: December 3, 2006
Published online: May 11, 2007

 © 2007 Wiley-VCH Verlag GmbH & Co. KGaA, Weinheim